



ISSN: 0067-2904

Determination of Electrons Temperature and Density For Ag, Zn, and Cu metals using Plasma jet System at atmospheric pressure

Kadhim A. Aadim, Ghaith H. Jihad*

Department of Physics, College of Science, University of Baghdad, Iraq

Received: 30/7/2021

Accepted: 3/10/2021

Published: 30/5/2022

Abstract

Under atmospheric pressure, an argon plasma stream was sustained and its plasma characteristics were examined. The emission spectra of plasma created in a plasma jet system using argon gas were observed for three metals (Ag, Zn, and Cu) for the anode and varied flow rates ranging from 1–4 L/min. at constant voltage, and normal atmospheric pressure. The spectral lines of excited Ar, Ag, Zn, and Cu species were identified at a wavelength of (650–900) nm. The Debye length, sphere, and temperature of an electron are all measured. Optical emission spectrometer (OES) equipment was used to capture the spectrum produced by the plasma at various argon gas flow rates. The temperature and density of the electron (T_e) and (n_e) ranges for Ar-gas, Ag, Zn, and Cu-anode increased as the stream pace of argon gas to the plasma made by the release current (D.C.) expanded. (1.241- 1.473)eV and (1.93×10^{18} – 6.38×10^{18}) cm^{-3} , (1.187– 1.245) eV and (4.32×10^{16} – 6.23×10^{16}) cm^{-3} , (1.374 -1.631)eV and (4.01×10^{18} – 12.1×10^{18}) cm^{-3} respectively. The intensity of spectral lines, on the other hand, increased.

Keywords: Cold atmospheric pressure plasma jet (APPJs), Argon gas (Ar), Silver (Ag-metal), Zinc (Zn-metal), copper (Cu-metal) spectral characterization

ايجاد درجة حرارة وكثافة الالكترن لمعادن كل من الفضة , الزنك والنحاس بوساطة منظومة بلازما النفث في ظروف الضغط الجوي

كاظم عبد الواحد عادم ، غيث هادي جهاد*

قسم فيزياء، كلية العلوم، جامعة بغداد، بغداد، العراق

الخلاصة

في ظروف الضغط الجوي ، تم توليد بلازما النفث و فحص خصائصها البلازمية. تم استخدام نفثة البلازما للحصول على خصائص البلازما المتولدة في وسط مائي منزوعة الأيونات التي تحتوي على معادن مختلفة باستخدام تدفق غاز Ar عبر الإبرة. تحت الضغط الجوي العادي ، وبجهد ثابت ، وبمعدلات تدفق تتراوح من 1-4 لتر / دقيقة ، حيث تمت دراسة خصائص البلازما المتولدة من غاز الأركون المنبعث . وتم تحديد الخطوط الطيفية لكل من Ar و Ag و Zn و Cu المثارة وبمدي يتراوح بين 650 و 900 نانومتر. حيث تم دراسة وحساب كل من طول ديبي ، عدد الجسيمات في كرة ديبي ، ودرجة حرارة الإلكترون. تم التقاط الطيف الناتج عن البلازما بمعدلات تدفق غاز الأرجون المتنوعة باستخدام معدات مطياف الانبعاث البصري (OES). تم حساب كل من درجة حرارة وكثافة الإلكترون (Te) و (ne) لكل من Ar-gas

*Email: ghaith.jihad1104@sc.uobaghdad.edu.iq

و Ag-metal و Zn-metal و Cu-metal حيث ارتفع معدل تدفق غاز الأرجون إلى البلازما الناتج عن تيار التفريغ (DC). (1.241- 1.473) الكتلون-فولت و (1.93×10^{18} - 6.38×10^{18}) سم³ , (1.187- 1.245) الكتلون-فولت و (4.32×10^{16} - 6.23×10^{16}) سم³ , (1.374 -1.631) الكتلون-فولت و (4.01×10^{18} - 12.1×10^{18}) سم³ على التوالي , حيث لوحظ زيادة شدة الخطوط الطيفية مع زيادة تدفق ضغط الغاز .

1-Introduction

[1]. Atmospheric pressure plasma jet (APPJ) is a non-thermal plasma. It has acquired a lot of interest because of its flexibility, its ability to create reactive chemical temperatures in addition of its low-cost operation[1]. An interesting feature of APPJs is their capacity to infiltrate and spread inside little openings and adaptable dielectric tubes [2]. These facts make the plasma jet very attractive for applications in the biomedical field. Delivery of cold plasma through a flexible tube in a specific location can be very useful for endoscopic applications in medicine, such as the treatment of colorectal and pancreas cancers [3,4].

Plasma Jet is a promising technique used for generating cold atmospheric pressure glow plasma. Cold atmospheric pressure plasma is utilized widely in a variety of plasma processing methods, including surface modification of various materials, medical application, air treatment, water treatment, gas treatment [5].

To spectrally resolve and detect plasma light, a spectrograph and a detector are needed. The plasma spectrum that results can give quantitative and qualitative data, such as element composition. Emission line lengths, forms, and variations of the plasma spectrum can tell you about the temperature of the plasma and the density of electrons[6]. Plasma temperature is a crucial thermodynamic parameter because it may be used to define and forecast other plasma properties such as relative energy level populations and particle speed distribution. The ratio technique with two lines of hydrogen was employed in this work which presupposes that local thermodynamic equilibrium (LTE) is attained inside the plasma. Estimates show that LTE is typically achieved within a few hundred nanoseconds after plasma arrangement utilizing laser induced breakdown spectroscopy (LIBS) with higher irradiances of 10^8 W/cm² in vacuum with pressures up to 2.5×10^{-2} mbar.

A typical approach for determining plasma temperature is the intensity ratio of two spectral lines from a similar ionization stage of an atom or ion, the plasma temperature in local thermal equilibrium is given by the following equation [7]:

$$T_e = \frac{(E_2 - E_1)}{k \ln \left(\frac{I_1 \lambda_1 A_2 g_2}{I_2 \lambda_2 A_1 g_1} \right)} \dots \dots \dots (1)$$

Where E_1 is the energy of first line in the spectrum of plasma, E_2 is the energy of second line in the spectrum of plasma, k is boltzmann constant, I_1 is the intensity of first line, I_2 is the intensity of second line, $A_1 g_1$ is the transition strength of the first line and $A_2 g_2$ is the transition strength of the second line. Density of electrons (n_e) refers to the quantity of free electrons per unit volume. Plasma spectroscopy, microwave and laser interferometry, and Thomson scattering are some of the techniques used to determine electron density. The technique used in this work to determine electron density is the linear Stark broadening of spectral lines. Line broadening in APPJ is caused primarily by Doppler width and the Stark effect. The temperature and atomic mass of the emitting species determine Doppler width; this sort of widening is ignored in this experiment because the Doppler width of the hydrogen line utilized is typically between 0.04 and 0.07 nm.

The Stark effect is a form of pressure broadening that occurs when radiators and adjacent particles interact. Collisions of ions and to a lesser extent, electrons, create these interactions in plasmas. The widening of the hydrogen line utilized in this experiment is primarily due to the Stark effect [6,8].

In the Saha-Boltzmann equation, the same element's spectral lines and successive ionization phases are utilized [7]. The following is the Saha-Boltzmann equation:

$$n_e = \frac{I_1}{I_2^*} 6.04 \times 10^{21} (T)^{3/2} e^{\frac{(E_1 - E_2 - X_z)}{kT}} \text{ (cm}^{-3}\text{)} \dots\dots\dots(2)$$

Where

$$I_2^* = \frac{I_2 \lambda_2}{g_2 A_2} \dots\dots\dots(3)$$

X_z is the species ionization energy during the ionization stage, E in eV, T_z denotes the line force as it descends from level-2 to level-1, and T_e is the electron temperature. The addendum z represents the species' ionization phase for the reference. On the other hand, the plasma frequency is calculated using the following equation:

$$f_p \approx 8.98 \sqrt{n_e} \text{ (Hz)} \dots\dots\dots(4)$$

One of the essential characteristics of plasma is its frequency, which is solely dependent on the plasma density. [9]

Debye shielding is the response of charged particles to lower local electric fields, and it is this shielding that gives plasma its quasi-neutrality feature. λ_D often known as the Debye length, is defined as [10]:

$$\lambda_D = \left(\frac{\epsilon_0 k T_e}{n_e e^2} \right)^{1/2} = 743 * (T_e / n_e)^{1/2} \dots\dots\dots(5)$$

where :- λ_D is the Debye length (cm), n_e is the number of electrons, T_e is the electron temperature, e is the electron charge (C), and N_D is the number of particles in the Debye sphere, which is dependent on electron density and temperature [11]. As shown in [12], N_D [1] is the second need for plasma presence.

$$N_D = \frac{4\pi}{3} n_e \lambda_D^3 \dots\dots\dots(6)$$

2-Experimental Setup

2.1 Plasma jet system

Using an atmospheric plasma jet, cold plasma was created with varying argon gas flow rates at a fixed voltage. Plasma technology is made up of the following parts:

- Ar-gas which is employed for the production of cold plasma..
- A gas flow meter, with a range of about (1-4)L/min, to measure the gas intake and it is linked to a hollow metal tube.
- Cu, Ag, and Zn sheet metal with a 3 cm length.
- High voltage (D.C.) power supply of voltage between (10 to 14) kV

2.2 Experiment setup

Figure 1: shows a flowchart illustrating the processes involved in this research.

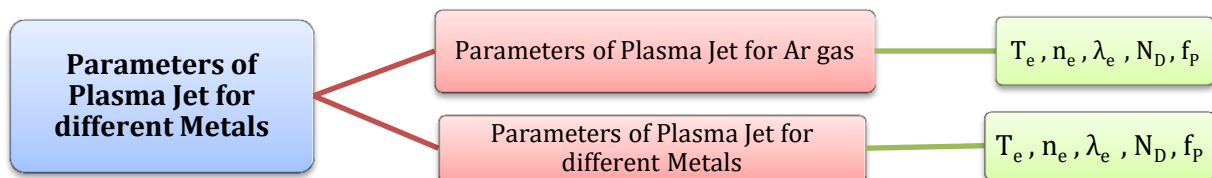


Figure 1- Scheme of the experimental work of the plasma jet

One of the most successful oxidation approaches for polluted water cleanup is the cold plasma jet. A gas that has been electrically charged by passing it through a strong electric field is referred to as a non-thermal plasma jet. The bulk of the electric field energy is employed to form energetic plasma species rather than just heating the gas. These species include positive

ions, electrons, negative ions, free radicals, electrically neutral gas atoms, molecules, and electromagnetic radiation. Plasma species are powerful oxidizers that break down organic and inorganic pollutants in the environment when they come into contact with contaminated media and mix with them.

In this work, Ar-gas with different flow rates was used. The high voltage power supply was designed to give about (10-14)kV. The anode was made of three distinct metals (Ag, Zn, and Cu). Figure 2 shows the configuration of D.C. atmospheric Plasma Jet system.

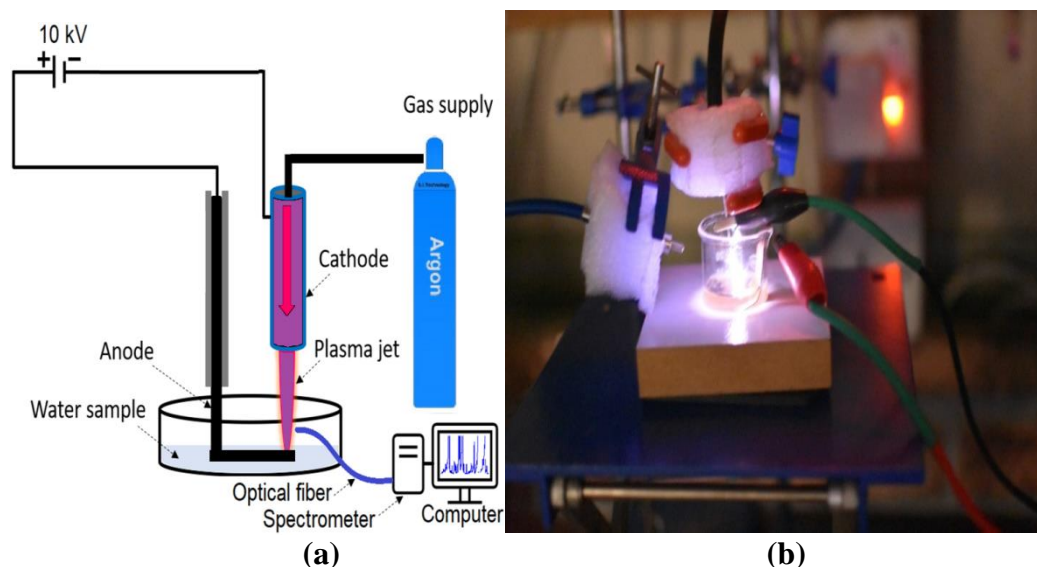


Figure 2- a) A schematic diagram of DC plasma jet with accompanying optical emission spectroscopic diagnosis. b) The plasma jet system configuration during the OES diagnostic procedure.

At 3,648 pixels responding to a range of the wavelength from (200-900)nm, the spectrometer offers a high resolution. Within a wavelength range of 690–780 nm, the spectra of Ar plasma for the three anode metals and for various gas flow rates were discovered. Finally, the findings were evaluated and compared to data from the National Institute of Standards and Technology (NIST)[13] in order to determine plasma parameters.

3-Results and Discussion

3.1 Calculation of plasma parameters

3.1.1 Optical emission spectroscopy(OES)

The plasma jet device recorded plasma emissions generated at atmospheric pressure at varied flow rates. The amplitude distribution spectrum that resulted was then plotted versus wavelength. The spectra of the optical emission of argon gas cool plasma were recorded using the OES method. A spectrum is made up of spectral lines that are unique to each atom and Ar ions (Figures (3-5)), in comparison to crisp standard lines for ArI and ArII, show the outflow spectra of argon gas with different metals of the anode to create cold plasma in the center frequency range of (685-900) nm with stream rates of (1-4) L/min. The OES method was used to record the optical emission spectra of Ar, Ag, Zn, and Cu. Figures 3-5 show that the flow rate of argon has a consistent and substantial effect on the emission line intensities. The intensity of the spectral lines grow as the gas flow rate increases i.e. as more molecules move through the tube. The vast majority of gas molecules that pass through the plasma needle ionize the gas that passes through it, increasing the number of excited atoms and, as a result, a spectral line intensity peak is registered on the spectrum.

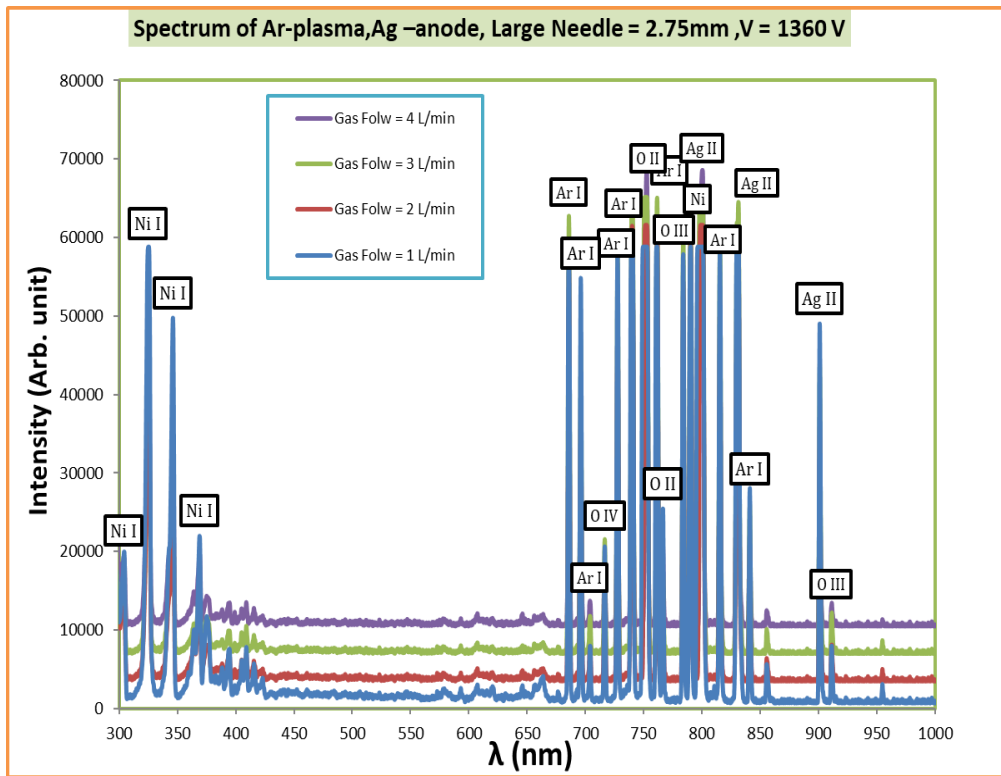


Figure 3-Cold plasma spectrum at atmospheric pressure for Ag anode at different Ar gas flow rates.

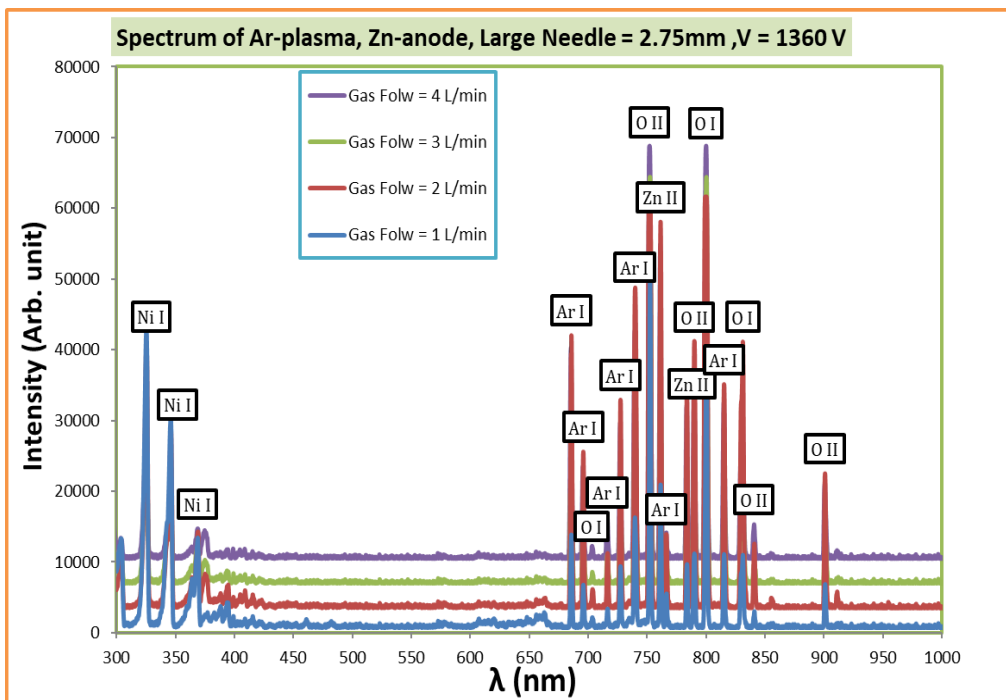


Figure 4-Cold plasma spectrum at atmospheric pressure for Zn anode at different Ar gas flow rates.

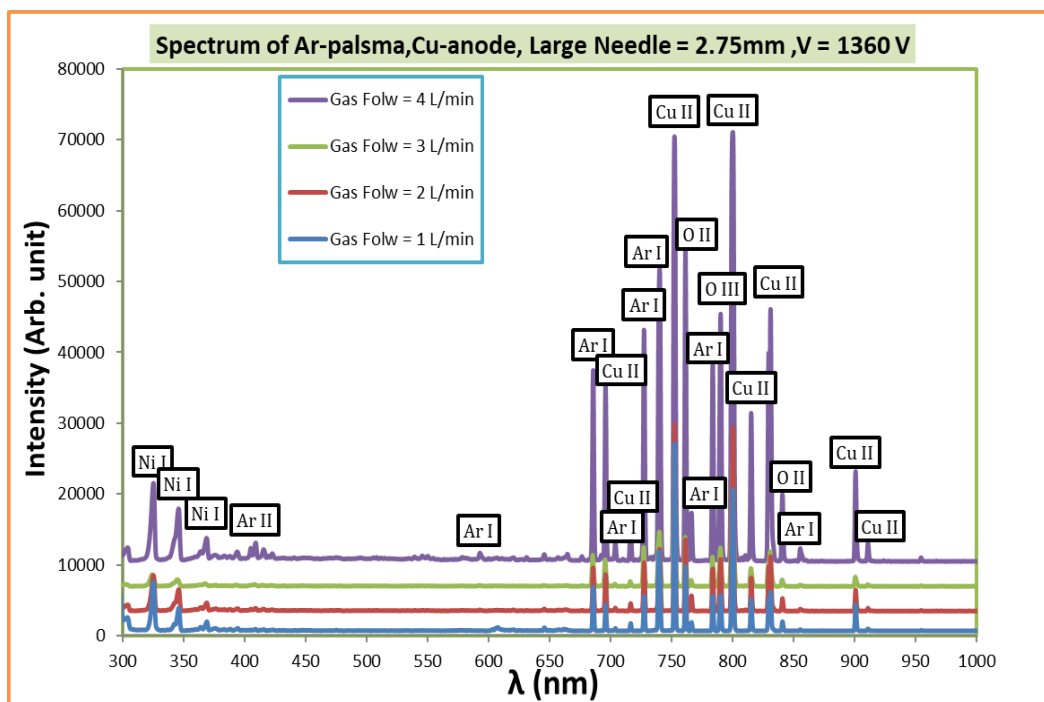


Figure 5-Cold plasma spectrum at atmospheric pressure for Cu anode at different Ar gas flow rates.

3.1.2 Evaluation of electron temperature and density

Figures 6–9 show how Eq (1) from the line strength ratio was used to determine the temperature of the electron (T_e); Using spectra from the OES, the relevant upsides of a few barriers were obtained from the NIST data set [13]. In Eq. 1, the Saha–Boltzmann equation (Eq.(2)) was used and the measured electron temperature and the electron density were determined.

The graph in the figures depicts the effect of a change in gas flow rate on the temperature (T_e) and density (n_e) of the electron. As seen [14] T_e and n_e in the cold plasma system grow by increasing the flow rate. At 1 L/min flow rate, electron temperature and density are 1.241 eV and $1.93 \times 10^{18} \text{ cm}^{-3}$, respectively, but at 4 L/min, the values are 1.473 eV and $6.38 \times 10^{18} \text{ cm}^{-3}$, respectively.

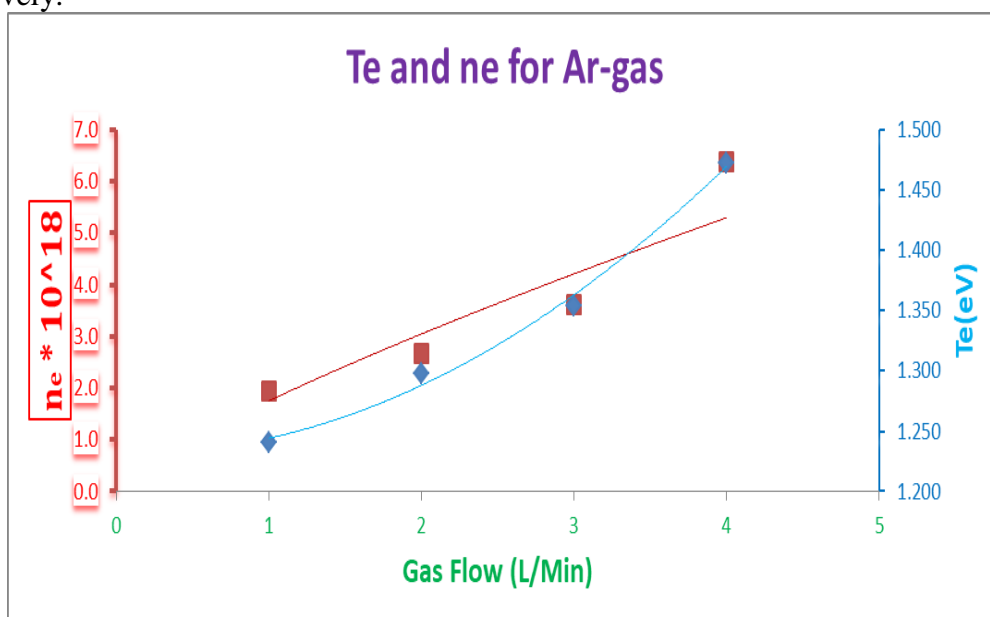


Figure 6 -Electron temperature and density for Ar-gas as a function of gas flow rate.

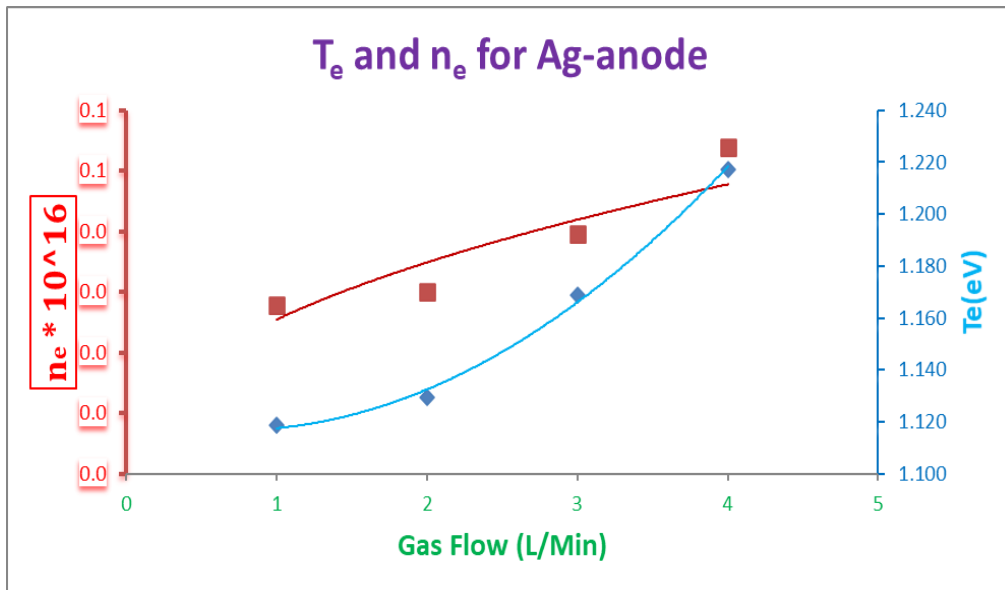


Figure 7-Changes of electron temperature and density as a function of gas flow rate for Ag-anode.

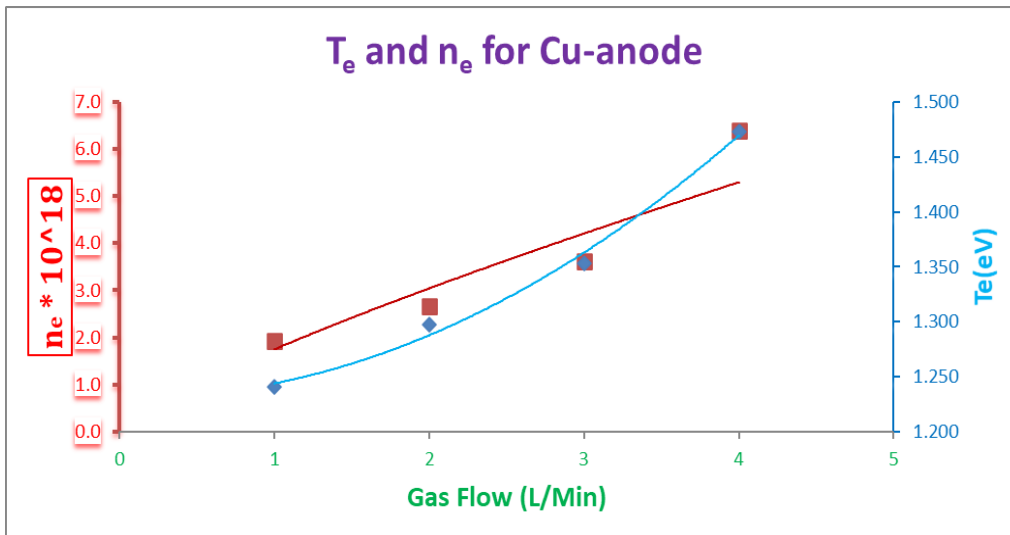


Figure 8-Changes of electron temperature and density as a function of gas flow rate for for Cu-anode.

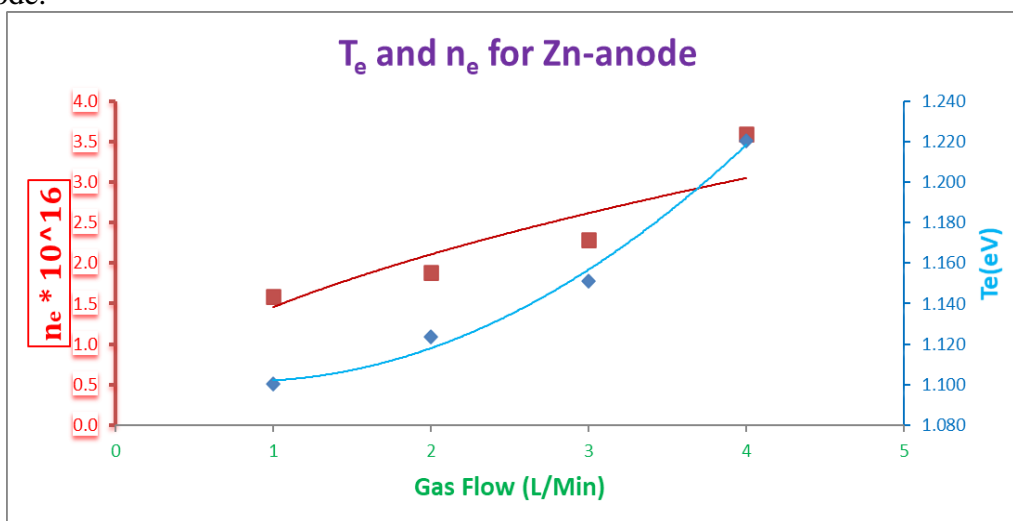


Figure 9- Changes of electron temperature and density as a function of gas flow rate for Zn-anode.

Tables (1-4) list the electron temperature (T_e), the electron density (n_e), plasma frequency (f_p), Debye length (λ_D), and Debye number for Ar gas and Ar-plasma at various flow rates and for the different metals used for the anode. From these, (N_D) was calculated for the different flow rates. The plasma requirements were met by all computed plasma parameters (λ_D , f_p , and N_D). It demonstrates that f_p decreases as the laser energy increases since it is proportional to n_e , But N_D has the reverse tendency; it increases with the decrease of n_e . This is consistent with the findings of Aadim [15].

Table 1- Plasma properties at varied flow rates (L/min) of Ar gas

Flow rates (L/Min)	T_e (eV)	n_e (cm^{-3}) $\times 10^{18}$	f_p (Hz) $\times 10^{13}$	λ_D (cm) $\times 10^{-5}$	N_D $\times 10^6$
4	1.473	6.38	2.3	3.3	0.97
3	1.353	3.61	1.7	4.2	1.1
2	1.297	2.67	1.5	4.8	1.2
1	1.241	1.93	1.2	5.5	1.4

Table 2- Ag anode plasma characteristics at various flow rates (L/min)

Flow rates (L/Min)	T_e (eV)	n_e (cm^{-3}) $\times 10^{16}$	f_p (Hz) $\times 10^{12}$	λ_D (cm) $\times 10^{-4}$	N_D $\times 10^6$
4	1.245	6.23	2.2	3.1	7.7
3	1.196	4.59	1.9	3.5	8.4
2	1.176	4.01	1.8	3.7	8.8
1	1.187	4.32	1.9	3.6	8.6

Table 3- Zn anode Plasma characteristics at various flow rates (L/min).

Flow rates (L/Min)	T_e (eV)	n_e (cm^{-3}) $\times 10^{16}$	f_p (Hz) $\times 10^{12}$	λ_D (cm) $\times 10^{-4}$	N_D $\times 10^6$
4	0.785	2.91	1.5	3.6	5.6
3	0.756	1.91	1.2	4.3	6.5
2	0.744	1.59	1.1	4.7	7.0
1	0.734	1.35	1.0	5.1	7.4

Table 4- Cu anode plasma characteristics at various flow rates (L/min)

Flow rates (L/Min)	T_e (eV)	n_e (cm^{-3}) $\times 10^{18}$	f_p (Hz) $\times 10^{13}$	λ_D (cm) $\times 10^{-5}$	N_D $\times 10^6$
4	1.631	12.1	3.1	2.5	0.82
3	1.499	7.16	2.4	3.2	0.94
2	1.437	5.42	2.1	3.6	1.0
1	1.374	4.01	1.8	4.0	1.1

4-Conclusions

It was found that the intensity of cold plasma emission spectra lines produced by a plasma jet is greatly dependent on external circumstances. According to the data, the increase in the emission intensity of the spectrum produced by the argon gas passage shows that the number of gas molecules is growing. This indicates that the energy of the electrolyte field is strong enough to cause secondary ionization of molecules, ionizing the vast majority of gas particles passing through the plasma tube. As a result, the flowing gas turns into plasma, with the lowest force and maximum power at 1 L/min and 4 L/min, respectively. It was concluded that the increase of the gas flow rate has a substantial impact on plasma properties such as electron density and temperature. The Debye length, the recurrence of plasma, and the number of particles on Debye's surface all rise as the gas stream rate increases.

5-References

- [1] X. Lu, M. Laroussi, V. Puech, "On atmospheric-pressure non-equilibrium plasma jets and plasma bullets," *Plasma Sources Sci Technol.*, vol. 21, no. 3, pp.777-788, 2012.
- [2] V. S. Johnson, W. D. Zhu, R. Wang, J. L. Re, S. Sivaram, J. Mahoney, J. L. Lopez, "A cold atmospheric-pressure helium plasma generated in flexible tubing," *IEEE Trans Plasma Sci.*, vol. 39, no. 11, pp. 2360-2361, 2011.
- [3] E. Stoffels, J. Contrib. *Plasma Phys.*, vol. 47, no. 1-2, pp. 40-48, 2007.
- [4] E. Robert, M. Vandamme, L. Brullé, S. Lerondel, A. Le Pape, V. Sarron, D. Riés, T. Darny, S. Dozias, G. Collet, C. Kieda, J. M. Pouvesle, *J. Clin. Plasma Medicine*, vol. 1, no. 2, pp. 8-16, 2013.
- [5] M. M. Hameed , Abdul-Majeed E. Al-Samarai and K. A. Aadim, "Synthesis and Characterization of Gallium Oxide Nanoparticles using Pulsed Laser Deposition," *Iraqi Journal of Science*, vol. 61, no. 10, pp. 2582-2589, 2020.
- [6] David A. Cremers, *Handbook of Laser-Induced Breakdown Spectroscopy*, 2nd Editio. USA, 2013.
- [7] S. Z. H. R. and J. A. Kashif Chaudhary, "Laser-Induced Plasma and its Applications," *RFID Technol. Secur. Vulnerabilities, Countermeas.*, 2016.
- [8] D. K. Naser , A. K. Abbas and K. A. Aadim, "Zeta Potential of Ag, Cu, ZnO, CdO and Sn Nanoparticles Prepared by Pulse Laser Ablation in Liquid Environment," *Iraqi Journal of Science*, 2020, Vol. 61, No. 10, pp: 2570-2581.
- [9] M. C. Chen and E. C. Chen, *Introduction To Plasma Physics And Controlled Fusion*, vol. 1. Los Angeles, 1983.
- [10] A. M. El Sherbini and A.A.S. AlAamer, "Measurement of Plasma Parameters in Laser-Induced Breakdown Spectroscopy Using Si-Lines," *World J. Nano Sci. Eng.*, vol. 2, no. 4, pp. 206–212, 2012.
- [11] B. M. Smirnov, *Physics of Ionized Gases*, vol. 16, no. 1. 2001.
- [12] Suresh Chandra, *textbook of plasma physics*, 1ed ed. india, 2010.
- [13] version 5., "National Institute of Standards and Technology (NIST) Atomic spectra database," 2017.
- [14] Mazhir S N, Abdullah N A, Rauuf A F, Ali A H and Al-Ahmed H 2018 Effects of Gas Flow on Spectral Properties of Plasma Jet Induced by Microwave. *Baghdad Science Journal* Vol.15(1)81-86. <http://dx.doi.org/10.21123/bsj.2018.15.1.0081>.
- [15] K.A. Aadim, 2019, Spectroscopic studying of plasma parameters for SnO₂ doped ZnO prepared by pulse Nd:YAG laser deposition, *Iraqi Journal of Physics* 17(42), 125-123. Doi:10.20723/ijp.17.42.125-135.